# EEG Signal Recognition of VR Education Game Players Based on Hybrid Improved Wavelet Threshold and LSTM

Yang Li
School of Education Science, Minzu Normal University of Xingyi, China
woshiliyang88@126.com

Haiyu Zhang
School of Education Science, Minzu Normal University of Xingyi, China
Haiyu_Zhang.0715@outlook.com

**Abstract:** *According to Electroenc-Encephalo-Graphy (EEG) signal correlation analysis, attention levels of game players can objectively reflect changes in attention during Virtual Reality (VR) education games. To avoid noise interference, denoising processing is necessary. This study improves the traditional wavelet thresholding method by combining it with Ensemble Empirical Mode Decomposition (EEMD). Then, feature extraction is performed to remove noise and identify EEG features related to attention, which are classified using long short-term memory techniques. The proposed method is validated through experimental design, showing minimal root mean square error of 12.0231 and maximum signal-to-noise ratio of 11.3272, indicating effective denoising. In VR, attention is more focused and stable compared to the 3D environment. Time required to achieve challenge goals is 53.65 seconds in VR and 65.7 seconds in 3D environments, suggesting participants achieve goals earlier in VR. The correlation coefficient between VR and 3D environment is 0.784, indicating a strong correlation, with a Significant Difference (SD) in time required to achieve initial goals. The proposed method demonstrates effectiveness in EEG signal recognition.*

**Keywords:** *EEG signal, wavelet threshold method, LSTM, VR, EEMD.*

*Received May 27, 2024; accepted October 24, 2024*
*https://doi.org/10.34028/iajit/22/1/13*

## 1. Introduction

The most commonly used algorithm for recognizing electroencephalogram signals is Electroenc-Encephalo-Graphy (EEG). To improve the understanding and feature processing of EEG signals, wavelet threshold method is often used. Wavelet threshold is a method of signal denoising that can eliminate correlation coefficients below the threshold. The traditional wavelet threshold may exhibit pseudo-Gibbs phenomenon at discontinuous points of the signal during the denoising process, and the selection of threshold has a significant impact on the denoising effect [19]. This study combines Ensemble Empirical Mode Decomposition (EEMD) with wavelet thresholding method, resulting in a higher signal-to-noise ratio and the ability to obtain purer EEG signals. EEMD is a specific algorithm used to solve the problem of modal mixing, which can remove noise from EEG signals and is particularly suitable for processing nonlinear signals [26]. Then, this study used Long and Short-Term Memory (LSTM) to balance the efficiency of feature classification of EEG signals. Traditional feature classification methods typically represent them as sparse vectors, while LSTM models can be represented as dense vectors to capture more semantic information [11]. The LSTM model can take word vectors as input, extract features through the LSTM layer, and finally input the obtained features into the fully connected layer for classification. This study combines EEMD with improved wavelet thresholding to preprocess EEG signals, then performs feature extraction and uses LSTM for feature classification; this played an important role in the later research of EEG signals. The article structure is as follows: The first part elaborates on the research background and significance of EEG signal recognition and related algorithms; the second part focuses on the process of combining the improved wavelet threshold method and EEMD algorithm in this research design, and using LSTM to classify and optimize the features of EEG signals. This part is also the focus and innovation of this study; The third part elaborates on the experimental verification on the ground of the algorithm designed in the second part and the quantitative analysis of the experimental data results; The fourth part draws conclusions on the experimental results and elaborates on the shortcomings of this design; Further in-depth directions are needed in the future.

## 2. Related Works

EEG recognition is one of the emerging topics that has attracted attention. Generally, this EEG based recognition is an effective model for many real-time applications. There have been many studies on EEG recognition, and Wei *et al*. [25] proposed an EEG

classification technique based on multidimensional fusion features to solve the problems of poor performance, low efficiency, and poor robustness of EEG signals generated by brain sensory motor activation tasks. The results indicate that this method has good effectiveness in EEG signal processing. Chai and Ba [3] created a system that uses EEG signals to identify psychological stress caused by auditory and visual stimuli. To solve the problem that spatial uniform sampling methods cannot accurately reflect the dynamic characteristics of multivariate EEG signals, a non-uniform sampling algorithm is proposed. This algorithm adaptively selects the projection direction using the Duffing equation, and research has shown that the algorithm has the characteristics of efficient convergence speed. To improve the overall rate of emotion recognition in emotion classification systems, Jiang *et al*. [12] proposed a CSP-VAR-CNN (CVC) system for emotion recognition. This system utilizes Common Spatial Patterns (CSP) to reduce the amount of EEG data and selects normalized Variance and R (VAR) as a parameter to create emotion feature vectors. Then it uses Convolutional Neural Networks (CNNs) algorithm to classify the emotions of EEG signals, and constructs a 5-layer CNN model to classify EEG signals. The results indicate the superiority of constructing a model for processing EEG signals. Wankhade and Doye [24] use advanced tools and models to detect human emotions or feelings through EEG signals. To effectively represent EEG signals, a descriptive Emerging Market Credit Derivatives (EMCD) and wavelet transform with 2501 features were applied, and then these features were used in Deep Trust Networks (DBN) classifiers to classify emotions. This study indicates that it has reference value for sensitive expression of human emotions. Bakhshali *et al*. [2] proposed a method for classifying EEG signals of imagined speech, which is both high-precision and efficient. To achieve this, the distance between matrices is used as a metric for imaginative speech recognition, and the correlation spectral density matrix of EEG signals is evaluated on different channels. Statistical methods are used to evaluate channel selection and frequency band detection in imagined speech. Priyadarshini and Reddy [17] team proposed an adaptive neurofuzzy inference system classifier for automatic detection of seizures. It uses discrete wavelet transform to analyze the EEG signal filtered by Finite Impulse Response (FIR) to extract relevant features for the proposed classifier to learn. It improves classification accuracy by using binary particle swarm optimization algorithms to select the optimal features. The proposed classifier was optimized and better results were obtained. To effectively solve the classification problem of EEG signals, Meng *et al*. [14] proposed a recursive mapping CNN motion image classification algorithm. The first step of this algorithm is to use preprocessing technology to enhance the signal strength within the motion range. The second step is to extract frequency domain and time domain features, and use them to construct recursive map feature patterns. This study indicates that the developed new neural network can accurately recognize left and right movements.

Many scholars have improved the wavelet threshold denoising for processing EEG signals. Chen [4] improved the original wavelet denoising method by innovatively mixing soft and hard thresholds instead of the previous single threshold judgment. This enhances the denoising algorithm, achieving correct recognition of English speech signals, and also amplifies the signal-to-noise ratio of English speech recognition, while reducing the root mean square error of the signal. The results verified that it achieved a significant reduction in noise and greatly improved the accuracy of speech recognition. Parija *et al*. [16] used an effective optimization algorithm, the water circulation algorithm, to optimize kernel parameters for diagnosing and classifying epileptic EEG signals. An improved hybrid model is proposed by combining Empirical Mode Decomposition (EMD) features with weighted multi kernel random vector function linked networks. The experiment shows that the model has excellent performance in efficient recognition and classification of EEG signals. Tuncer *et al*. [22] proposed a new abnormal EEG signal detection model using Chaotic Local Binary Pattern (CLBP) and Wavelet Packet Decomposition (WPD) techniques. Firstly, the study used chaotic feature generation functions to perform WPD on EEG signals, and then applied CLBP to the decomposed signals to extract features. Then it uses a support vector machine classifier to classify these features to distinguish between normal and abnormal EEG categories. The results indicate that the accurate classification of normal and abnormal EEG signals is valuable for EEG signal processing and medical diagnosis. Liu *et al*. [13] proposed a method of using motion detection to locate the position of people in tunnels. This algorithm uses a three plane method based on bilateral ranging to achieve localization. Using wavelets to analyze motion signals to separate low-frequency and high-frequency signals, in order to determine the impact of motion noise on Ultra-Wide-Band (UWB) positioning. Use soft threshold function and hard threshold function to perform wavelet thresholding denoising on the motion localization results of the tunnel. The results show that the method has a 94% accuracy in identifying and locating positions. Tong *et al*. [21] proposed a signal denoising method for Microchip Electrophoresis devices using Capacitive Coupled non-Contact Conductivity Detection (ME-C-4D). This method adopts an improved wavelet threshold function, which effectively removes electronic interference in ME-C-4D analog signals while preserving the peak shape and area. This study shows that the denoising purity of this method is efficient in dealing with signal interference.

In summary, in the research of EEG signal recognition, EEG is usually used and combined with relevant algorithms such as CNNs. The most commonly used recognition method for processing EEG signals is wavelet threshold denoising. Many studies have made corresponding improvements to wavelet denoising, but the depth of research on combining EMD with improved wavelet threshold denoising is not deep. This study will process EEG signals on the ground of improved wavelet thresholding and EEMD followed by feature extraction and classification using machine learning and deep learning techniques; Finally, it uses long-term and short-term memory to balance the efficiency of classified EEG signals and the classification results. The summary of Related Work is shown in Table 1.

Table 1. Summary table of related work.

| Ref. | Author | Technology | Result |
|---|---|---|---|
| [25] | Wei *et al*. | Improved Morlet wavelet, 3D CNN, Bi GRU model | Propose EEG classification technology based on multidimensional fusion features |
| [3] | Chai and Ba | Non uniform sampling algorithm, Duffing equation | Create a system to identify psychological stress caused by audio-visual stimuli |
| [12] | Jiang *et al*. | CSP, VAR, CNN | Propose CVC system for emotion recognition |
| [24] | Wankhade and Doye | EMCD, Wavelet transform, DBN classifier | Detecting human emotions using EMCD and wavelet transform |
| [2] | Bakhshali *et al*. | Related spectral density matrix, statistical methods | Propose a high-precision and efficient method for classifying imaginative speech EEG signals |
| [17] | Priyadarshini and Reddy | Discrete wavelet transform, FIR filtering, binary particle swarm optimization algorithm | Propose an adaptive neural fuzzy inference system classifier for automatic detection of epileptic seizures |
| [14] | Meng *et al*. | Preprocessing techniques, recursive map feature patterns | Propose a recursive mapping CNN algorithm for motion image classification |
| [4] | Chen | Hybrid threshold denoising for English speech recognition | Improve wavelet denoising method by mixing soft threshold and hard threshold |
| [16] | Parija *et al*. | EMD, Weighted multi kernel random vector function linked network | Optimization of EMD features and weighted multi-core random vector function linked network using water cycle algorithm |
| [22] | Tuncer *et al*. | CLBP, WPD, SVM classifiers | Propose an abnormal EEG signal detection model based on CLBP and WPD |
| [13] | Liu *et al*. | Three plane method based on bilateral ranging, wavelet analysis, soft threshold function, and hard threshold function | Proposed a method of using motion detection to locate the position of people in tunnels |
| [21] | Tong *et al*. | Wavelet threshold function | Proposed a signal denoising method |

## 3. Research on LSTM Combined with Improved Wavelet Threshold for Player EEG Signal Recognition

This study involves feature extraction and selection of EEG waves, which require denoising of the collected EEG waves. Improved wavelets are used to denoise EEG signals and then extract features and classify them; Finally, it uses long-term and short-term memory to balance the results of classified EEG waves, making it easy to observe and understand.

### 3.1. Fusion of Wavelet Thresholding and Set Empirical Mode Decomposition for EEG Signal Processing

EEG waves exist throughout human life, and brain computer interaction involves directly extracting EEG signals from the cerebral cortex and analyzing them to achieve mechanical control. The Brain Computer Interface (BCI) serves as a bridge for brain computer interaction. With the development of bioscience and neuroscience, it has been confirmed that EEG signals collected from the human scalp can clearly and objectively reflect a person's attention level, reflecting the instantaneous changes in attention state during the experimental process through EEG signals. EEG signals are often distinguished on the ground of frequency, and the characteristics of different frequency bands have been thoroughly studied [1, 7].

Figure 1 demonstrates that the collected EEG signal needs to be amplified and converted into a digital signal through a digital to analog converter. When collecting EEG signals, there may be noise [6, 9]. To avoid noise interference in subsequent research, it is necessary to perform denoising processing. Then feature extraction can be performed, which also requires removing noise and identifying EEG features related to attention. Then, machine learning and deep learning techniques are used to classify them.

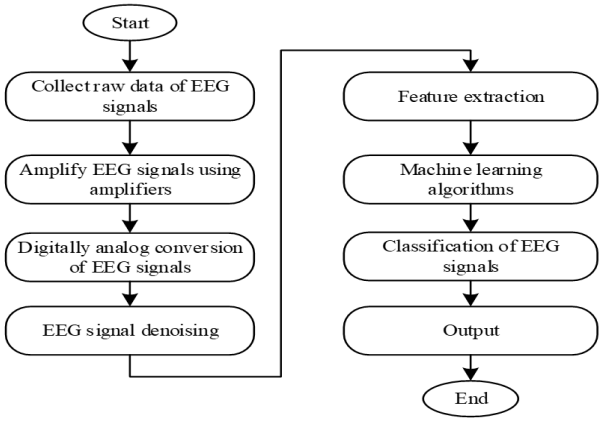


Figure 1. EEG signal analysis flowchart.

Due to the extremely weak EEG signal and complex operation of brain neurons during brain computer interaction, significant interference may occur during the EEG signal acquisition process. Along with known EMG, EOG, ECG, and power frequency signals,

additional unpredictable noise signals may appear, which can disrupt the accurate collected EEG signals and cause frequency band overlap [20, 28]. In existing research, the signal is inverted after passing through a bandpass or low-pass filter, thereby utilizing Fourier transform to reduce noise. Due to the complexity and variability of EEG signals, wavelet transform is difficult to adjust the basis and scale of their decomposition. This study has made corresponding improvements to the standard wavelet threshold denoising method.

Regarding the denoising problem of EEG signals, this study combines the traditional wavelet threshold denoising algorithm with EEMD denoising to improve it. This involves using a combination of EEMD and enhanced wavelet threshold technology to remove noise from the EEG signal and obtain a clean attention-based EEG signal [8, 29]. To solve the problem of modal mixing, a specific algorithm - the overall average EMD algorithm - was adopted, which can remove noise from EEG signals and is particularly suitable for processing nonlinear signals. It utilizes white noise to evenly distribute energy and improve signal stability, so that the signal can be accurately decomposed into scales. For EEG feature extraction, EEG features are an effective tool for describing signals. Feature extraction is usually divided into four categories: time-domain, frequency-domain, time-frequency analysis, and nonlinear features [18]. In the process of removing noise and processing features, although EEG signals are collected in a very quiet experimental environment, some forms of interference, such as power frequency signals and electrocardiograms, inevitably mix into the actual signal. To solve this problem, EEGLAB has its own toolbox that can help semi-automatically eliminate this noise. Figure 2 illustrates the process of automatically identifying and subsequently removing eye signals from collected EEG data.

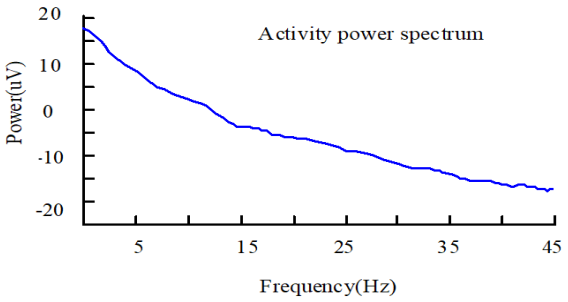


Figure 2. Removing eye electrical signals.

In the process of reducing noise, attention signals will also decrease. This is because noise and attention signals are not completely independent, and there are complex nonlinear disturbances between them within the frequency range. Wavelet transform can solve the problem of insufficient Fourier transform's ability to analyze frequencies at different times due to nonlinear interference. By performing Fourier transform on signals from all time periods, frequency information at different time points can be obtained. The transformation formula is shown in Equation (1).

$$STFT(t, f) = \int_{-\infty}^{\infty} \left[x(\tau)h(t-\tau)\right] e^{-j2\pi f\tau} d\tau \tag{1}$$

In Equation (1), the $h(t)$ function represents the time window function of the length of time. To solve the problem of inflexible time frame of short time Fourier transform and adapt it to the current problem, wavelet transform was introduced. Wavelet transform is used to determine frequency and time, and has attenuation characteristics. The wavelet transform formula is shown in Equation (2).

$$W_f(a,\tau) = \left\langle f, \psi_{a,b} \right\rangle = \frac{1}{\sqrt{a}} \int_{-\infty}^{+\infty} f(t) * \varphi\left(\frac{t-\tau}{a}\right) dt \tag{2}$$

In Equation (2), the scale $a$ and the translation $\tau$ are divided into frequency and time, which can control the scaling and translation of the wavelet function. Wavelet transform can ensure the effectiveness of the processed EEG signal. To evenly distribute the noise energy among all wavelet coefficients during the processing, Gaussian noise is usually used, and its distribution is not affected after the wavelet transform. The process of wavelet threshold denoising is divided into the following steps: performing wavelet decomposition on noisy signals, thresholding the obtained wavelet coefficients, and finally reconstructing the wavelet coefficients of each layer. The focus of wavelet threshold denoising is the selection of threshold functions, which can be divided into hard threshold and soft threshold methods. The hard threshold denoising method of wavelet is shown in Equation (3).

$$\tilde{W}_{j,k} = \begin{cases} 0, \left|W_{j,k}\right| \le \lambda \\ W_{j,k}, \left|W_{j,k}\right| > \lambda \end{cases} \tag{3}$$

The soft threshold denoising method of wavelet is shown in Equation (4).

$$\tilde{W}_{j,k} = \begin{cases} 0, \left|W_{j,k}\right| \le \lambda \\ \operatorname{sgn}\left(W_{i,k}\right)\left(\left|W_{j,k}\right| - \lambda\right), \left|W_{j,k}\right| > \lambda \end{cases} \tag{4}$$

The above two methods also have the following shortcomings: hard threshold denoising has signal oscillation, and soft threshold has constant error. This study has made relevant improvements to the wavelet threshold function in response to the problem. It introduces EMD, which is a signal analysis method. EMD has no basis function limitations and can be transformed into an adaptive decomposition algorithm [10]. The EMD method can be used to analyze physiological signals, with the main idea being the Internal Mode Function (IMF), which decomposes complex non-stationary signals into a finite number of

IMF. When the data meets local standards for maximum, minimum, and time scales, it can be decomposed into signals. When the conditions are met, the original signal is decomposed as shown in Equation (5).

$$x(t) = \sum_{i=1}^{n} imf_i(t) + r_n \tag{5}$$

In Equation (5), $x(t)$ represents the original signal; $r_n$ represents residual; $imf_i(t)$ represents each IMF component. The algorithm flow of EEMD is shown in Figure 3.

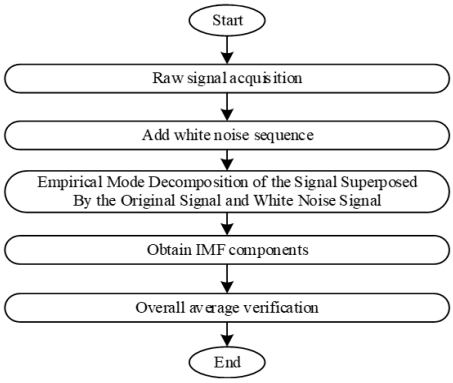


Figure 3. Algorithm flowchart of EEMD.

Figure 3 indicates that the white noise sequence is used to add different white noise to the original signal in each iteration, resulting in a set of IMF. These IMFs are combined and evenly divided, and after repeated averaging iterations, noise is eliminated, resulting in denoising results.

### 3.2. Research on the Performance of Improved Wavelet Threshold Denoising Algorithm in Processing EEG Signals

On the ground of the combination of wavelet threshold and EEMD denoising principle, the specific flowchart is shown in Figure 4. The noisy EEG is decomposed by EEMD to obtain IMF components with instantaneous frequency distribution from high to low. By improving the wavelet threshold function and combining it with EMD algorithm, the signal is denoised [27]. It uses EEMD to decompose the original signal into multiple scales, as in EEMD decomposition, denoising the entire original signal may reduce the effective signal due to the gradual reduction of IMF noise components. Then, the high-frequency signal is processed to implement an enhanced wavelet threshold algorithm, and ultimately reconstructed using low-frequency components.

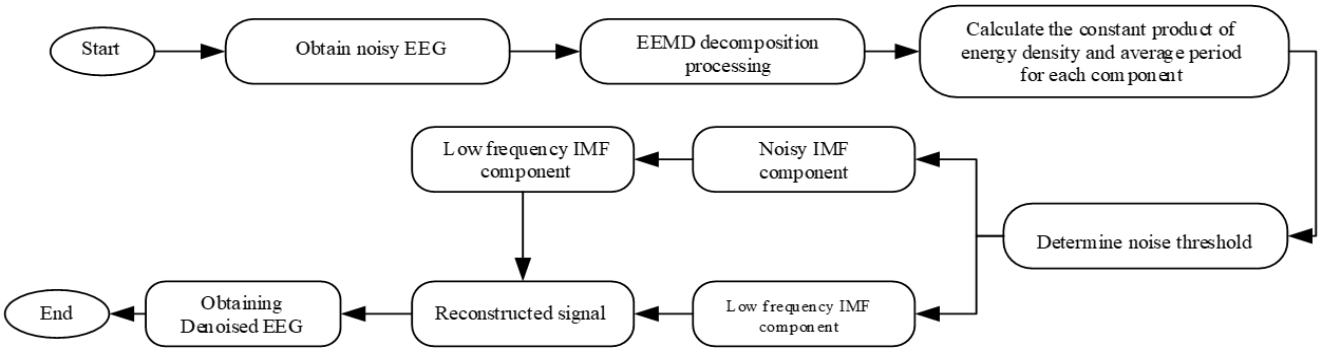


Figure 4. EEMD and improved wavelet threshold denoising flowchart.

By decomposing complex signals into smaller parts, the key components containing noise in the IMF are determined. After EEMD decomposition, the constant product of energy density and average period in each IMF is used. By performing EEMD decomposition on the noisy raw signal, $M$ IMF components are obtained, representing the energy density and average period, as calculated in Equation (6).

$$\begin{cases} EN_i = \dfrac{1}{n}\sum_{j=1}^{n} imf_{i,j}^{\,2} \\ \bar{T} = \dfrac{2n}{D_i} \\ P_i = EN_i * \bar{T} \end{cases} \tag{6}$$

In Equation (6), $n$ is the length of each IMF component; $D_i$ is the total number of extreme points for the $i$-th IMF component. By implementing an enhanced wavelet threshold to remove noise from the initial $k$ IMF components, the improvement focuses on two key areas: minimizing the differences between signals and ensuring the continuity of the new threshold function in the wavelet space. The improved algorithm proposed in this study is shown in Equation (7).

$$\tilde{W}_{j,k} = \begin{cases} 0, \left|W_{j,k}\right| \le \lambda \\ \operatorname{sgn}\left(W_{i,k}\right)\left(\left|W_{j,k}\right| - \dfrac{\lambda}{e^{W_{j,k}^2 - \lambda^2}}\right), \left|W_{j,k}\right| > \lambda \end{cases} \tag{7}$$

When $W_{j,k} > 0$, as shown in Equation (8).

$$\lim_{W_{j,k}\to\infty} \frac{\tilde{W}_{j,k}}{W_{j,k}} = 1 - \frac{\lambda W_{j,k}}{e^{W_{j,k}^2 - \lambda^2}} = 1 \tag{8}$$

When $W_{j,k} < 0$, as shown in Equation (9).

$$\begin{cases} \lim\limits_{W_{j,k}\to\infty} \dfrac{\tilde{W}_{j,k}}{W_{j,k}} = 1 + \dfrac{\lambda W_{j,k}}{e^{W_{j,k}^2-\lambda^2}} = 1 \\ \lambda = \sigma\sqrt{2\ln N} \end{cases} \tag{9}$$

In Equation (9), $N$ represents the sequence length; $\sigma$ represents the standard deviation of noisy signals; $\widetilde{W}_{j,k}=W_{j,k}$ represents the improved asymptotic line, and for the new threshold function, $\frac{\lambda}{e^{W_{j,k}^2-y^2}}$ will gradually decrease as $W_{j,k}$ increases. The improved algorithms in existing research are shown in Equation (10).

$$\tilde{W}_{j,k} = \begin{cases} 0, |W_{j,k}| \le 0 \\ \mathrm{sgn}(W_{j,k})\sqrt{W_{j,k}^2 - \lambda^2}, |W_{j,k}| > \lambda \end{cases} \tag{10}$$

To verify the performance of the improved algorithm in processing data, it calculates the corresponding root mean square error and signal-to-noise ratio, as shown in Equation (11).

$$\begin{cases} R_{RMSE} = \sqrt{1/N \sum\limits_{i=1}^{N} (x_i - \hat{x}_i)^2} \\ S_{SNR} = 10\lg\left( \sum\limits_{i=1}^{N} x_i^2 \Big/ \sum\limits_{i=}^{N} (x_i - \hat{x}_i)^2 \right) \end{cases} \tag{11}$$

In Equation (11), $x_i$ represents the initial value of the original signal at time $i$; $x_i$ represents the reconstructed value at that time after denoising; $N$ represents the length of the signal sequence. The larger the signal-to-noise ratio, the better the root mean square difference, and the better the denoising effect. Power spectrum estimation is a general term for algorithms that estimate the power spectral density of random signal sequences. It belongs to one of the analysis methods that describe the characteristics of random signals in the frequency domain. It performs power spectrum analysis on EEG signals, as shown in Equation (12).

$$S(w) = \frac{1}{k} \sum_{i=1}^{k} \frac{\left| \sum\limits_{N=0}^{M-1} X^i(n) w(n) e^{-j\frac{2\pi}{N}kn} \right|}{\sum\limits_{N=0}^{M-1} w^2(n)} \tag{12}$$

The study first divided $N$ data points into $K$ segments, each with $M=N/K$ data points. This study multiplies segmented data $X(n)$ by window function $w(n)$ to obtain the power spectrum of each segment. It sums the power spectra of all segments and calculates the average value to obtain the final power spectrum estimation. Although estimating the power spectrum can intuitively reflect the power distribution in each rhythm, qualitative analysis can only be conducted on the changes in the main frequency bands involved in EEG energy feature transfer, and further quantification is needed. This study used the Burg method and AR model parameters for feature extraction when quantifying power spectral density features, as shown in Equation (13).

$$x(n) = -\sum_{i=1}^{p} a_p(i) x(n-i) + \varepsilon(n) \tag{13}$$

Equation (13) uses a difference equation to process the signal, where $x(n)$ represents the EEG sequence; $\varepsilon(n)$ represents white noise. It uses the Brug method to estimate the AR model parameters, as shown in Equation (14).

$$\begin{cases} P = \dfrac{1}{2}\left( P_f + P_b \right) \\ P_f = \dfrac{1}{M-k} \sum\limits_{n=k}^{M-1} \left| e_k^f(n) \right|^2 \\ P_b = \dfrac{1}{M-k} \sum\limits_{n=k}^{M-1} \left| e_p^b(n) \right|^2 \end{cases} \tag{14}$$

In Equation (14), $M$ represents the signal length; $P_f$ represents forward error power; $P_b$ represents the backward error power; $P$ represents the sum of prediction error power.

### 3.3. Application of EEG Signal Extraction and VR Environmental Attention Research Using LSTM as a Classifier

After classifying EEG signals, it is also necessary to balance efficiency and classification results. This study used a deep learning LSTM classifier. LSTM is an important model of machine learning algorithms, as shown in Figure 5 for its overall structure and the specific structure of a neuron. Due to the influence of the previous time on the input and output of LSTM, there are three inputs of LSTM at time $t$: $x_t$, $h_{t-1}$ and $C_{t-1}$, which are the current time, the output value of the previous time, and the current state unit. Compared to traditional cyclic CNNs, LSTM performs better in long sequence problems [23].

Attention refers to the guidance and concentration of specific objects by psychological activities or consciousness, which can be seen as the ability of consciousness to concentrate and indicate the level of attention. Figure 6 is a schematic diagram of the structure of the human body information processing system. Figure 6 shows that individuals receive external stimuli through their senses, process the obtained information under the influence of attention, and then make decisions and reactions. Attention can significantly affect a person's working memory, and the input, encoding, storage, and retrieval of information require careful attention. The ability to maintain attention to specific goals in daily life is crucial for achieving advanced cognition.

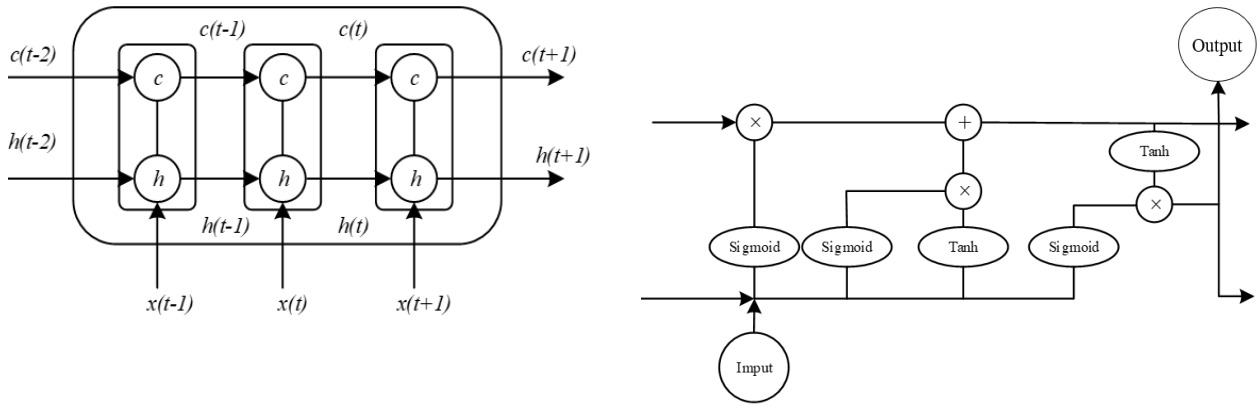


a) Overall structure diagram. b) Neuron detail map.

Figure 5. EEMD and improved wavelet threshold denoising flowchart.

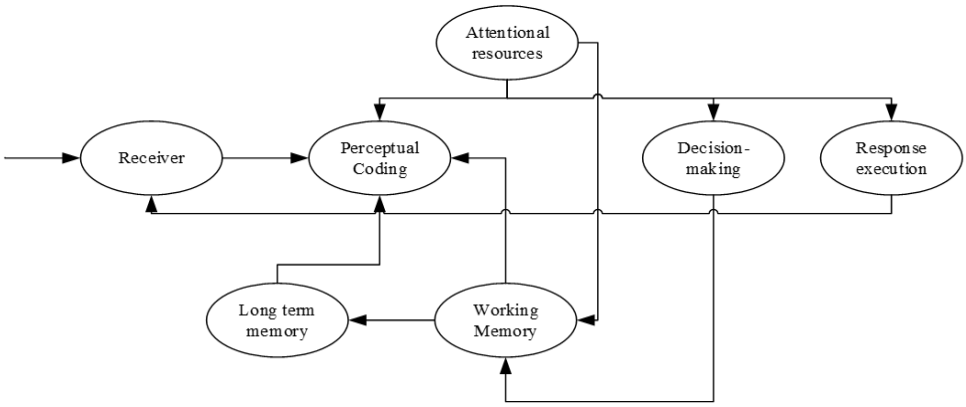


Figure 6. Structure diagram of human body information processing system.

The LSTM neural network divides the training data into three stages: forgetting stage, selective memory stage, and output stage [5, 15]. Each output of the sigmoid layer is a real number between 0 and 1, representing the weight that allows the corresponding information to pass through. In the forgetting stage, it focuses on selectively discarding inputs from the previous node. In addition, by using the calculated sigmoid layer as a forgetting gate, it is possible to control which information needs to be retained or discarded from the previous state $C_{t-1}$. It chooses the memory stage. The input at this stage has selective "memory", mainly focusing on basic information while selecting and memorizing the input text. The output stage will generate the current state. This study uses the activation function tanh to scale the state values of the previous stage. Compared to standard RNNs, LSTM can execute more effectively in longer sequences. Due to the limited nature of ordinary neural networks, which can only process inputs one by one, each input is independent and independent of previous or subsequent inputs, it is not suitable for processing EEG signals. In addition, ordinary RNNs have problems with gradient vanishing and gradient explosion. Therefore, using LSTM neural networks to process EEG signals is more suitable.

It studies whether there is a Significant Difference (SD) in game performance between players in Three-Dimensional (3D) and Virtual Reality (VR) game settings. It uses recorded pitches and hit rates as the basis for analyzing game performance, and uses hit rate $d$ to measure participants' performance in different game environments in subsequent data processing. It assigns a number between 1 and 10 to the obtained $d$ value for precision and interval mapping, calculated as Equation (15).

$$\begin{cases} d = \dfrac{N}{M} \\ y = \dfrac{y_{\max} - y_{\min}}{x_{\max} - x_{\min}} * (x - x_{\min}) + y_{\min} \end{cases} \tag{15}$$

In Equation (15), $M$ represents the number of throws recorded by the experimental subject in the VR task; $N$ represents the number of hits. $x$ is any value of the current data; $y$ is the value after normalization mapping; $x_{\min}$ and $x_{\max}$ represent the minimum and maximum values of the current data, respectively; $y_{\max}$ and $y_{\min}$ represent the maximum and minimum values of the target interval, respectively.

## 4. Verification and Testing of Hybrid Wavelet Threshold Improvement and Attention Study of LSTM EEG Signals in Game Environment

This study denoises the collected EEG waves, uses improved wavelet combined with EEMD to denoise the

EEG signals, and then extracts features and classifies them; Finally, it uses long-term and short-term memory to balance the results of classified EEG waves, and designs experiments to verify the performance and feasibility of the proposed method.

## 4.1. Preparation and Design of Experimental Data

This experiment will start with preprocessing and denoising, and then extract EEG signals using power spectrum estimation, sample entropy, and Hilbert Huang transformation specifically targeting attention related signals. Sample entropy and approximate entropy have similar physical meanings, both measuring the complexity of a time series by measuring the probability of generating new patterns in a signal. The higher the probability of generating new patterns, the greater the complexity of the sequence. Hilbert Huang transform, including EEMD and Hilbert Spectrum Analysis (HSA), is an effective signal analysis method. It combines traditional support vector machines and deep learning algorithms in pairs to classify features. The advantages and disadvantages of two classification algorithms were compared. On the ground of the existing requirements and status of attention EEG, the EEG device used in this experiment has a data sampling rate of 256Hz, which can collect 16 channels of EEG signals and create virtual scenes using HTC VIVE. Due to the significant decrease in EEG signals after passing through the skull and sebum, signal amplification is necessary to obtain observable and analyzable EEG signals. As shown in Figure 7, there are a total of 16 channels for the placement of some electrodes.

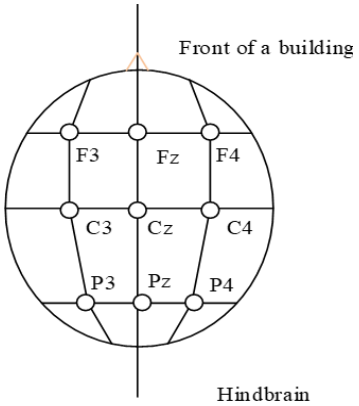


Figure 7. Partial electrode placement position.

The attention classification experiment uses traditional digital game experiments (Schulte grid) to classify attention and EEG signal processing methods. This experiment collected EEG signals from 20 mental health participants aged 22 to 26, with a gender ratio of 1:1 (10 males and 10 females). All participants did not receive attention related training. Table 2 shows the scores obtained by some participants in the game when experiencing two environments. The composition of game performance data includes the probability of participants hitting targets in different environments and the time required to complete the challenge for the first time. The analysis of participants using paired sample t-tests and independent sample tests to test game performance data.

Table 2. Scores obtained by some participants experiencing games.

| Subject number | 3D Game score | VR Game score | Exchange or not |
|---|---|---|---|
| 1 | 1.48 | 5.36 | / |
| 2 | 3.18 | 6.25 | / |
| 3 | 5.94 | 7.26 | / |
| 4 | 7.21 | 10 | / |
| 5 | 3.18 | 5.98 | / |
| 6 | 1.2 | 2.64 | Yes |
| 7 | 2.97 | 5.47 | Yes |
| 8 | 2.15 | 3.84 | Yes |
| 9 | 2.32 | 2.65 | Yes |
| 10 | 3.48 | 8.47 | Yes |

The experiment obtained a dataset of 1280*16*1080, consisting of 16 channels of EEG data from 360 high attention states, 360 normal attention states, and 360 non attention states, with 1280 sampling points per segment (256Hz*5s).

Figure 8 shows the raw EEG signals collected during the data collection phase of the experiment.

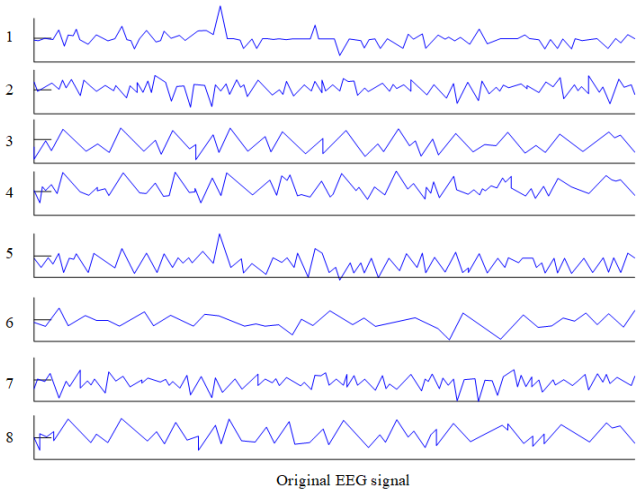


Figure 8. Original EEG signal.

## 4.2. Measurement and Analysis of Experimental Results

During the experiment, the EEMD and improved wavelet threshold denoising algorithm proposed in this study were compared with the EEMD and improved wavelet lifting algorithm. The following will take the high attention EEG data of F3 channel as an example in Figure 9, which indicates that the algorithm in this study has a better effect on denoising details.

After collecting EEG information, the experiment preliminarily separates the EEG patterns and extracts EEG rhythms before extracting features. It will use the signals obtained from wavelet decomposition for further research. The decomposition results are shown in Figure 10, which are beta wave, alpha wave, theta wave, and delta wave from top to bottom.

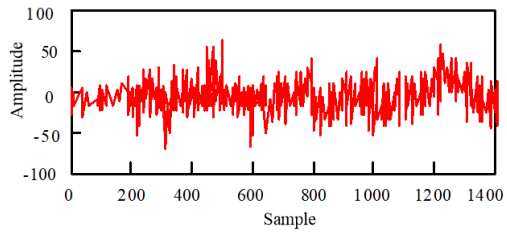


a) EEMD and improved wavelet threshold denoising algorithm.

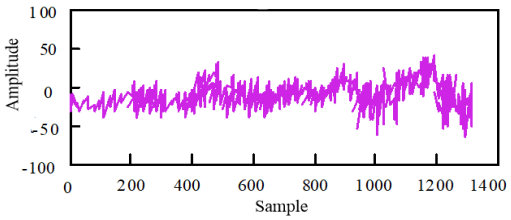


b) EEMD and improved wavelet lifting denoising algorithm.

Figure 9. Comparison of EEMD and wavelet denoising algorithms before and after improvement.

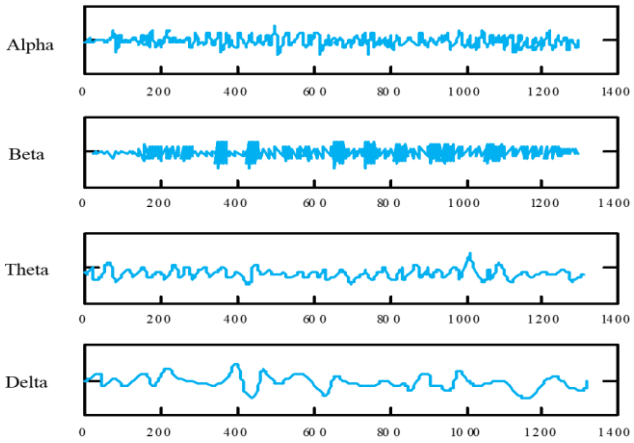


Figure 10. EEG signal maps of four rhythms.

To further validate the performance of the proposed algorithm, the root mean square error and signal-to-noise ratio were compared with traditional wavelet threshold denoising, EEMD denoising, EEMD and improved wavelet lifting algorithms. This indicates that the proposed method has the smallest RMSE of 12.0231 and the highest signal-to-noise ratio of 11.3272. The larger the signal-to-noise ratio, the better the root mean square difference, and the better the denoising effect.

Table 3 also provides detailed information on paired sample t-tests. In VR and 3D settings at a 90% confidence level, the chance value of t-test is P=4.12e-4<0.05. Two sets of correlations indicate that the correlation coefficient in VR and 3D gaming environments has a positive value of 0.784; This means that there is a strong correlation between paired samples, with a corresponding significance probability of P=2.48e-4<0.05. This indicates that there is a SD in the time required for participants to achieve their initial goals between the two environments, and there is a statistically SD.

Table 3. Comparison of root mean square error and signal-to-noise ratio of several algorithms.

| Algorithm | Number of experimental samples | RMSE | SNR |
|---|---|---|---|
| Algorithm denoising in this study | 20 | 12.0231 | 11.3272 |
| Traditional wavelet threshold denoising | 215 | 16.0215 | 4.4153 |
| EEMD denoising | 20 | 13.6989 | 7.943 |
| EEMD and improved wavelet lifting algorithm | 20 | 12.6184 | 9.9328 |

Power spectral density can display the frequency changes of EEG signals at different levels of attention. The use of power spectral density analysis is on the ground of biomedical research, typically analyzing power spectral density using flat band average power spectrum as a basis for evaluating attention deficit disorder. Power is not the main source of electrical activity, making it difficult to complete the attention process and leading to characteristics such as lack of concentration. Although the activity levels of individual brain centers may vary, the overall trend of attention activity remains consistent. As shown in Figure 11, it compares the power spectral density of F3 channels in the beta, alpha, theta, and delta bands under three different states, namely non attention state, normal attention state, and high attention state.

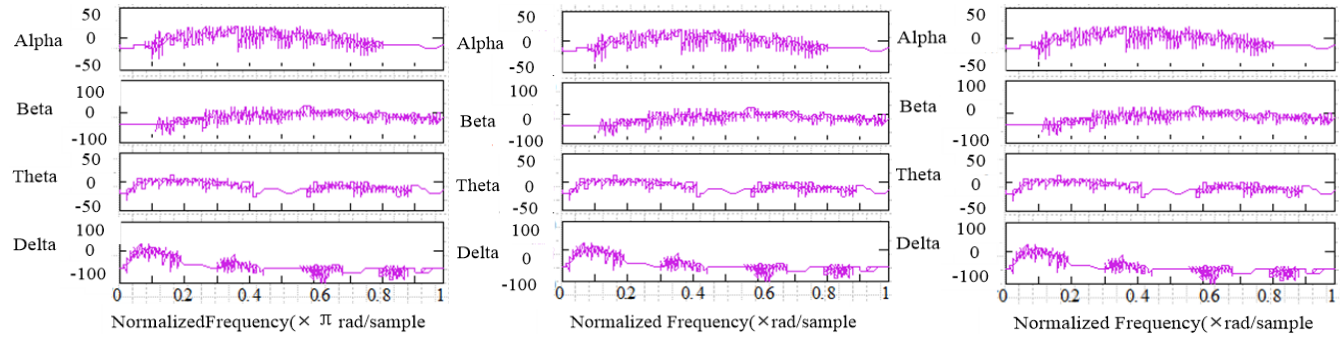


a) Non-attentional state. b) High attentional state. c) Normal attentional state.

Figure 11. Power spectral density of four waves in three states.

Figures 11-a), (b), and (c) show that when the subject is not paying attention, the power spectral density of alpha waves is higher than that of beta waves, and both remain at a constant level without significant change. When entering a highly focused state, the power value of the beta wave significantly increases, while the alpha wave shows a clear downward trend, and the theta and delta bands show irregular changes and an overall

downward trend. When transitioning from a high attention state to a normal attention state, alpha and theta waves become higher before gradually decreasing and stabilizing, while beta wave patterns decrease and stabilize, and theta waves appear to decrease.

Table 4 shows the time required to achieve challenge goals for the first time in VR and 3D environments, and compares the evaluation indicators of 3D and VR game time. In the VR game environment, it took 53.65 seconds, and in the 3D environment, it took 65.7 seconds, indicating that the subjects were able to complete the game objectives earlier in the VR environment. Table 3 also provides detailed information on paired sample t-tests. In VR and 3D settings at a 90% confidence level, the chance value of t-test is P=4.12e-4<0.05. Two sets of correlations indicate that the correlation coefficient in VR and 3D gaming environments has a positive value of 0.784; This means that there is a strong correlation between paired samples, with a corresponding significance probability of P=2.48e-4<0.05. This indicates that there is a SD in the time required for participants to achieve their initial goals between the two environments, and there is a statistically SD.

Table 4. Comparison of evaluation indicators for VR game and 3D game time.

| / | VR games | 3D games | VR games and 3D games |
|---|---|---|---|
| **Mean value** | 53.65 | 65.7 | -12.1 |
| **Number** | 20 | 20 | 20 |
| **Standard deviation** | 13.245 | 13.098 | 9.951 |
| **Mean standard error5** | 2.9845 | 3.0899 | 2.197 |
| **Upper limit** | / | / | -16.57 |
| **Lower limit** | / | / | -7.658 |
| **t** | / | / | -5.47 |
| **Freedom** | / | / | 18 |
| **Sig (Double tailed)** | / | / | 4.12E-04 |
| **Correlation** | / | / | 0.784 |
| **Significance** | / | / | 2.48E-04 |

In the experiment, the attention scores of all subjects were obtained within 90 seconds, and the data was processed to obtain the mean and standard deviation, as shown in Figure 12. This indicates that compared to the 3D environment, the subjects' attention is more focused in the VR environment, and the attention level in the VR environment is more stable and less volatile. Overall, compared to subjects in a 3D environment, people in a VR environment tend to be more focused. These results indicate that VR games can have a positive impact on attention levels.

In the experiment, two subjects were selected to observe the changes in attention levels over a period of 90 seconds in the 3D and VR task groups. Figure 13 shows the changes in attention scores of subject A in VR and 3D gaming environments. From the curve trend, there is no SD in attention scores between the two subjects in the two environments over a period of 5 to 20 seconds. However, after 25 seconds, the attention score in the VR environment showed an upward trend, while the attention score in the 3D environment remained relatively stable. This indicates that the attention score curves of subject B in both 3D and VR tasks show a gradual upward trend, indicating that their attention levels are steadily increasing from the beginning of the game to entering the attention state. Subjects participating in VR game tasks are most focused around 50 seconds, while those participating in 3D game tasks reach their highest point of attention around 75 seconds. The VR environment can also help subject B achieve higher levels of attention. Both 3D and VR gaming environments exhibit a trend of fluctuating around a specific value over a period of time while maintaining a certain level of stability.

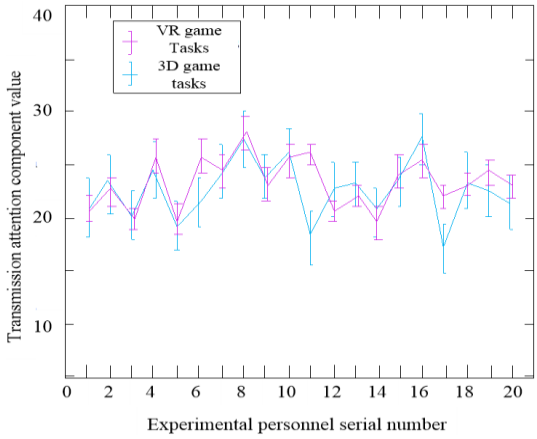


Figure 12. Subjects pay attention to the average score and standard deviation in 3D and VR.

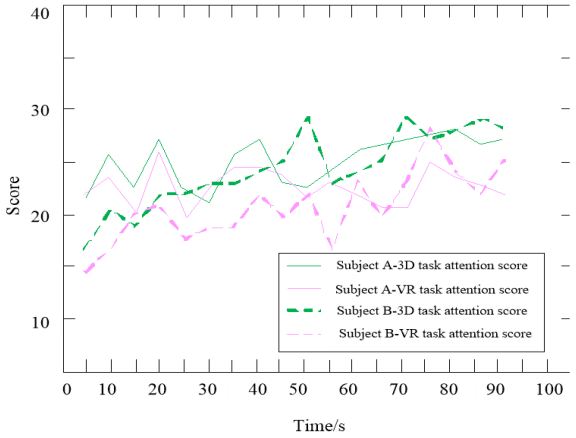


Figure 13. Comparison of EEG attention score change curves between subjects A and B.

## 5. Conclusions

It improves the wavelet thresholding method for denoising EEG signals, combined with the EEMD method to improve the efficiency of denoising, preserving the core parts of the signal, and then performs feature extraction. The classified EEG signal features are balanced between efficiency and classification results through LSTM. The design experiment verifies the proposed method, and the experiment shows that when the subject's attention is

not focused, the power spectral density of alpha waves is higher than that of beta waves, and both remain at a constant level without significant changes. When entering a highly focused state, the power value of the beta wave significantly increases, while the alpha wave shows a clear downward trend, and the theta and delta bands show irregular changes and an overall downward trend. When transitioning from a high attention state to a normal attention state, alpha and theta waves become higher before gradually decreasing and stabilizing, while beta wave patterns decrease and stabilize, and theta waves appear to decrease. Compared with traditional wavelet threshold denoising and EEMD denoising for root mean square error and signal-to-noise ratio, the proposed method has the smallest root mean square error of 12.0231 and the highest signal-to-noise ratio of 11.3272; This indicates that the denoising effect is good. Compared to the 3D environment, the subjects' attention in the VR environment is more focused, and the attention level in the VR environment is more stable with less fluctuations. This indicates the effectiveness and advantages of the algorithm studied in EEG signal processing. However, this study has not yet been comprehensively considered in different age, gender, and other populations, and further research is needed.

## Funding

The research is supported by: Doctoral Foundation Project of Minzu normal University of Xingyi, (No.20XYBS01).

## References

[1] Ahmad I., Zhang S., Saminu S., Wang L., Isselmou A., Cai Z., Javaid I., Kamhi S., and Kulsum U., "Deep Learning Based on CNN for Emotion Recognition Using EEG Signal," *WSEAS Transactions on Signal Processing*, vol. 17, pp. 28-40, 2021. https://wseas.com/journals/articles.php?id=329

[2] Bakhshali M., Khademi M., Ebrahimi-Moghadam A., and Moghimi S., "EEG Signal Classification of Imagined Speech Based on Riemannian Distance of Correntropy Spectral Density," *Biomedical Signal Processing and Control*, vol. 59, pp. 101899, 2020. https://doi.org/10.1016/j.bspc.2020.101899

[3] Chai M. and Ba L., "Application of EEG Signal Recognition Method Based on Duffing Equation in Psychological Stress Analysis," *Advances in Mathematical Physics*, vol. 2021, no. 1, pp. 1-10, 2021. https://doi.org/10.1155/2021/1454547

[4] Chen Z., "Signal Recognition for English Speech Translation Based on Improved Wavelet Denoising Method," *Advances in Mathematical Physics*, vol. 2021, no. 1, pp. 1-9, 2021. https://doi.org/10.1155/2021/6811192

[5] Cheng X. and Zhang P., "Enhanced Soccer Training Simulation Using Progressive Wasserstein GAN and Termite Life Cycle Optimization in Virtual Reality," *The International Arab Journal of Information Technology*, vol. 21, no. 4, pp. 549-559, 2024. DOI: 10.34028/iajit/21/4/1

[6] Cheng X., Mao J., Li J., Zhao H., Zhou C., Gong X., and Rao Z., "An EEMD-SVD-LWT Algorithm for Denoising a Lidar Signal," *Measurement*, vol. 168, no, 3, pp. 108405, 2021. https://doi.org/10.1016/j.measurement.2020.108405

[7] Dao F., Zeng Y., and Qian J., "A Novel Denoising Method of the Hydro-Turbine Runner for Fault Signal Based on WT-EEMD," *Measurement*, vol. 219, no. 1, pp. 1-16, 2023. https://doi.org/10.1016/j.measurement.2023.113306

[8] Dong Y. and Ren F., "Multi-Reservoirs EEG Signal Feature Sensing and Recognition Method Based on Generative Adversarial Networks," *Computer Communications*, vol. 164, no. 6, pp. 177-184, 2020. https://doi.org/10.1016/j.comcom.2020.10.004

[9] Ge J., Niu T., Xu D., Yin G., Wang Y., "A Rolling Bearing Fault Diagnosis Method Based on EEMD-WSST Signal Reconstruction and Multi-Scale Entropy," *Entropy*, vol. 22, no. 3, pp. 290-291, 2020. DOI: 10.3390/e22030290

[10] Jana G., Sabath A., and Agrawal A., "Capsule Neural Networks on Spatio-Temporal EEG Frames for Cross-Subject Emotion Recognition," *Biomedical Signal Processing and Control*, vol. 72, pp. 1-16, 2022. DOI:10.1016/j.bspc.2021.103361

[11] Javidan M., Yazdchi M., Baharlouei Z., and Mahnam A., "Feature and Channel Selection for Designing a Regression-based Continuous-Variable Emotion Recognition System with two EEG Channels," *Biomedical Signal Processing and Control*, vol. 70, no. 7, pp. 102979, 2021. https://doi.org/10.1016/j.bspc.2021.102979

[12] Jiang H., Wang Z., Jiao R., and Jiao S., "Picture-Induced EEG Signal Classification Based on CVC Emotion Recognition System," *Computers, Materials and Continua*, vol. 65, no. 2, pp. 1453-1465, 2020. DOI:10.32604/cmc.2020.011793

[13] Liu N., Zhang R., Su Z., Fu G., and He J., "Research on Wavelet Threshold Denoising Method for UWB Tunnel Personnel Motion Location," *Mathematical Problems in Engineering*, vol. 2020, no. 1, pp. 1-14, 2020. https://doi.org/10.1155/2020/9039648

[14] Meng X., Qiu S., Wan S., Cheng K., and Cui L., "A Motor Imagery EEG Signal Classification Algorithm Based on Recurrence Plot Convolution Neural Network," *Pattern Recognition Letters*, vol. 146, no. 4, pp. 134-141, 2021. DOI:10.1016/j.patrec.2021.03.023

[15] Naser D. and Saha G., "Influence of Music Liking on EEG Based Emotion Recognition," *Biomedical Signal Processing and Control*, vol. 64, pp. 1-15, 2021. DOI:10.1016/j.bspc.2020.102251

[16] Parija S., Dash P., and Bisoi R., "Multi-Kernel Based Random Vector Functional Link Network with Decomposed Features for Epileptic EEG Signal Classification," *IET Signal Process*, vol. 14, no. 3, pp. 162-174, 2020. https://doi.org/10.1049/iet-spr.2019.0277

[17] Priyadarshini B. and Reddy D., "Optimized Adaptive Neuro Fuzzy Inference System (OANFIS) Based EEG Signal Analysis for Seizure Recognition on FPGA," *Biomedical Signal Processing and Control*, vol. 66, no. 8, pp. 601-615, 2021. https://doi.org/10.1016/j.bspc.2021.102484

[18] Salankar N., Mishra P., and Garg L., "Emotion Recognition from EEG Signals Using Empirical Mode Decomposition and Second-Order Difference Plot," *Biomedical Signal Processing and Control*, vol. 65, no. 8, pp. 1-13, 2021. https://doi.org/10.1016/j.bspc.2020.102389

[19] Subasi A., Tuncer T., Dogan S., Tanko D., and Sakoglu U., "EEG-based Emotion Recognition Using Tunable Q Wavelet Transform and Rotation Forest Ensemble Classifier," *Biomedical Signal Processing and Control*, vol. 68, pp. 102648, 2021. https://doi.org/10.1016/j.bspc.2021.102648

[20] Thakran S., "A Hybrid GPFA-EEMD_Fuzzy Threshold Method for ECG Signal De-Noising," *Journal of Intelligent and Fuzzy Systems*, vol. 39, no. 5, pp. 6773-6782, 2020. DOI:10.3233/JIFS-191518

[21] Tong Y., Li J., Xu Y., and Cao L., "Signal Denoising Method Based on Improved Wavelet Threshold Function for Microchip Electrophoresis C4D Equipment," *Complexity*, vol. 2020, no. 1, pp. 1-11, 2020. https://doi.org/10.1155/2020/6481317

[22] Tuncer T., Dogan S., and Acharya U., "Automated EEG Signal Classification Using Chaotic Local Binary Pattern," *Expert Systems with Applications*, vol. 182, no. 1, pp. 115175, 2021. https://doi.org/10.1016/j.eswa.2021.115175

[23] Wang J., Sun Y., and Sun S., "Recognition of Muscle Fatigue Status Based on Improved Wavelet Threshold and CNN-SVM," *IEEE Access*, vol. 8, pp. 207914-207922, 2020. DOI:10.1109/ACCESS.2020.3038422

[24] Wankhade S. and Doye D., "Deep Learning of Empirical Mean Curve Decomposition-Wavelet Decomposed EEG Signal for Emotion Recognition," *International Journal of Uncertainty, Fuzziness and Knowledge-based Systems*, vol. 28, no. 1, pp. 153-177, 2020. https://doi.org/10.1142/S0218488520500075

[25] Wei M. and Lin F., "A Novel Multi-Dimensional Features Fusion Algorithm for the EEG Signal Recognition of Brain's Sensorimotor Region Activated Tasks," *International Journal of Intelligent Computing and Cybernetics*, vol. 13, no. 2, pp. 239-360, 2020. https://doi.org/10.1108/IJICC-02-2020-0019

[26] Wei P., Zhang J., Tian F., and Hong J., "A Comparison of Neural Networks Algorithms for EEG and sEMG Features Based Gait Phases Recognition," *Biomedical Signal Processing and Control*, vol. 68, pp. 102587, 2021. https://doi.org/10.1016/j.bspc.2021.102587

[27] Yu M., Xiao S., Hua M., Wang H., Chen X., Tian F., and Li Y., "EEG-based Emotion Recognition in an Immersive Virtual Reality Environment: From Local Activity to Brain Network Features," *Biomedical Signal Processing and Control*, vol. 72, pp. 1-13, 2022. DOI:10.1016/j.bspc.2021.103349

[28] Zhang S., Zhou L., Chen X. M., Zhang L., Li L., and Li M., "Network-Wide Traffic Speed Forecasting: 3D Convolutional Neural Network with Ensemble Empirical Mode Decomposition," *Computer-Aided Civil and Infrastructure Engineering*, vol. 35, no. 10, pp. 1132-1147, 2020. https://doi.org/10.1111/mice.12575

[29] Zhu J., Feng L., and Mo X., "Robust Multichannel EEG Signal Reconstruction Method," *Pattern Recognition Letters*, vol. 151, pp. 209-214, 2021. DOI:10.1016/j.patrec.2021.08.014

**Yang Li** obtained his Doctorate in Education from the Philippine Women's University in 2019. Currently, he serves as an Associate Professor at the School of Educational Science, Minzu Normal University of Xingyi. He has published over 30 research papers, five of which have been included in SCI, EI, and CPCI. His research interests include Artificial Intelligence, Educational Management, and Primary Education.

**Haiyu Zhang** obtained her Doctorate of Education degree from Philippine Women's University in 2022. Currently, she serves as an Associate Professor in the School of Educational Sciences at Minzu Normal University of Xingyi. She has published four national-level planned textbooks and more than 20 scientific research papers, among which two have been included in SCI, EI. Her research interests include Artificial Intelligence, Educational Management and Preschool Teacherss Language Education.